Reprinted from
Journal of Imaging Science and Technology® 65(5): 050404-1–050404-10, 2021.

Emphasis on Material Appearance by A Combination of Dehazing and Local Visual Contrast

Hiroaki Kotera▲
Kotera Imaging Laboratory, Chiba, Japan
E-mail: hiroimage@gmail.com

Abstract. *Material appearance is a perceptual phenomenon that the brain interprets from the retinal image. Though, it is not easy to analyze what features of optical images are effectively related to the stimulus inside the visual cortex. For this reason, an intuitive or heuristic approach has been taken to simulate the material appearance. The simulation results are expected to drive innovation for not only traditional craft or plastic arts industry but also more realistic picture displays on 4K/8K HDTV and Virtual Reality or Computer Graphics. Optical surface property of material is modeled by BRDF (Bidirectional Reflectance Distribution Function). Specular S and Diffusion D components are responsible for the "glossiness" and "texture" and are used to emphasize the material appearance by simply adjusting the mixing ratio. This study introduces the following two key models to emphasize the material appearance of a given image without using such measuring means as BRDF and discusses how they work individually and cooperatively. (1) α-based Dehazing model to emphasize clarity, wetness, gloss. (2) β-based Contrast model to emphasize texture, roughness. © 2021 Society for Imaging Science and Technology.*
[DOI: 10.2352/J.ImagingSci.Technol.2021.65.5.050404]

1. BACKGROUND

Human observers can recognize material property at a glance through sensory organs. Without touching materials, it can be concluded whether they would feel hard or soft, cool or warm, rough or smooth, wet or dry. Furthermore, it is possible to discern materials such as metal, wood, leather or cloth.

The material appearance is interpreted as a perceptual phenomenon of feeling or sensation that our brain perceives from optical image projected onto retina. It is still hard to untangle what information of the retinal image stimulates the visual cortex of V1–V5 and how it induces the material feeling in our brain. The mechanism of INNER VISION in brain is still a black box at present [1].

As a framework for material perception, Tsumura initiated the skin color appearance and proposed the concept of appearance delivering system [2].

In Brain Information Science research on *SHITSUKAN* (material perception) [3] by *MEXT* (*Ministry of Education, Culture, Sports, Science and Technology*) in Japan, the first stage (2010–2014 led by Dr. H. Komatsu) has finished and the second stage (2015–2019 led by Dr. S. Nishida) stepped forward into "multi-dimensional" material perception and currently, further research on "deep texture" is progressing. The results so far are being adopted by private companies and put onto practical use.

In spite of the complexity in material appearance mechanism, human sensations such as "gloss/matte", "transparent/translucent", "metal/cloth" are controllable by an intuitive but a smart technique.

For instance, Motoyoshi, Nishida, et al. [4] noticed the "***gloss***" perception appears when the luminance histogram is skewed. If it is stretched smoothly to the higher luminance, the object looks "***glossy***" but looks "***matte***", if compressed to the lower.

Sawayama and Nishida [5] developed "***wet***" filter by a combination of exponent-shaped TRC and boosted color saturation. It is interesting that any "***skew***" in the image features induces a sensational material perception. However, the mechanism why and how such sensations as "***gloss***" or "***wet***" are activated by the "***skew***" effect in INNER VISION is not untangled yet.

On the other hand, many R & D for practical applications are making steady progresses in private enterprises. As a typical successful example, a specular reflection control algorithm based on BRDF is implemented in LSI chip and mounted on a commercial 4K HDTV set [6].

The author recently announced a new model to transfer texture between objects of different materials by combining *LPT* (*Log Polar Transform*) and *PCM* (*Principal Component Matching*) [7].

2. KEY APPROACHES

Our daily scene visibility is degraded due to faint atmospheric pollution. Since any floating particle in the air disturbs the atmospheric transmittance, we never see the grand truth scenes even under clear sky. In previous studies, the author reported a basic *Dehazing* method [8] and improved *α-based Dehazing* model [9]. Usually, Dehazing is used for unveiling the heavy air pollution such as PM 2.5, but *α-based Dehazing* is applicable to daily natural scenes by adjusting the veiling factor α.

First, the *α-based Dehazing* was found to have the effect of emphasizing ***wetness*** and ***gloss*** as well as ***clarity***. The ***clarity*** is an important material appearance factor to give a clear transparent feeling. While, ***wetness*** and ***gloss*** may be

▲ IS&T Member.

Received May 25, 2021; accepted for publication Sept. 19, 2021; published online Oct. 18, 2021. Associate Editor: Samuel Morillas.
1062-3701/2021/65(5)/050404/10/$25.00

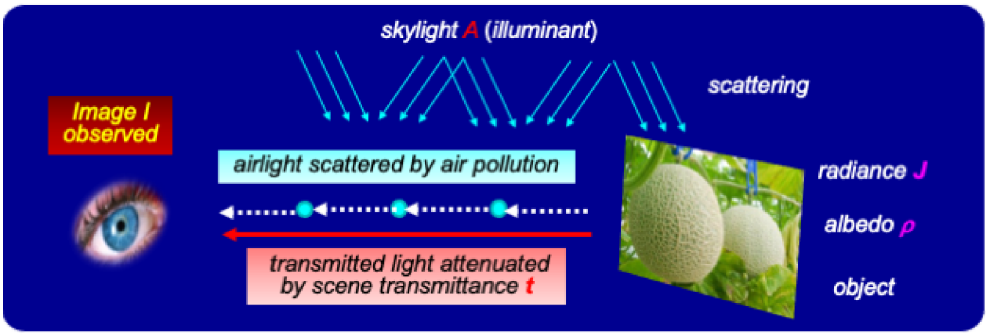

Figure 1. Hazy Image caused by Atmospheric Scattering.

a different feeling from ***clarity***, but are affected by *Dehazing* too. The idea of *Dehazing* seems to be a bit unconventional, but a challenging endeavor.

Second, the *β-based* local contrast operator, here we call *LCGT* (*Local Contrast Gain Transform*) [10] is tested for enhancing the "***textural***" appearance. *LCGT* is a spatially variant *TMO* (*Tone Mapping Operator*) based on *Weber's law*. Since *Weber fraction* is a vision-based measure of *JND* (*Just Noticeable Difference*), *LCGT* is designed suitable for visual contrast enhancement. It has been applied to Digital Video Camera [11] and HD Photo Printer [12], but not intended to material appearance. Here, it's shown how the ***texture*** *and* ***roughness*** are emphasized.

Finally, we introduce the material appearance enhancement effects by combining *α-based Dehazing* and *β-based LCGT*.

3. α-BASED DEHAZING MODEL

Figure 1 illustrates the composition of camera image through air floating particles based on atmospheric scattering physics [13].

The objective of Dehazing is to restore the albedo $\boldsymbol{\rho}$ by unveiling the scattered *airlight* from a single camera image $\boldsymbol{I}$.

A hazed camera image $\boldsymbol{I}(\boldsymbol{z})$ is described by

$$\boldsymbol{I}(\boldsymbol{z}) = \boldsymbol{J}(\boldsymbol{z})\boldsymbol{t}(\boldsymbol{z}) + (1 - \boldsymbol{t}(\boldsymbol{z})), \tag{1}$$

where, $\boldsymbol{J}(\boldsymbol{z}) = \boldsymbol{A}\boldsymbol{\rho}(\boldsymbol{z})$ and $\boldsymbol{t}(\boldsymbol{z}) = \exp^{-\sigma d(\boldsymbol{z})}$

σ = scattering coefficient $\cong$ constant for Mie scattering.

The 1st term denotes the direct transmission image from the scenic objects and the 2nd term means the *airlight* scattered from the *skylight* $\boldsymbol{A}$. The *skylight* $\boldsymbol{A}$ acts as a scene illumination and the *airlight* causes the hazy scene by veiling the direct transmission light. $\boldsymbol{J}(\boldsymbol{z})$ and $\boldsymbol{\rho}(\boldsymbol{z})$ denote the scene ***radiance*** and ***albedo***.

The scene transmittance $\boldsymbol{t}(\boldsymbol{z})$ is attenuated exponentially according to the scene depth $d(\boldsymbol{z})$. Note that $\boldsymbol{z} = (x, y)$ denotes each pixel coordinates in the 2-D camera image $\boldsymbol{I}(\boldsymbol{z})$ corresponding to the objects placed at scene depth $d(\boldsymbol{z})$.

A key to restore the albedo $\boldsymbol{\rho}(\boldsymbol{z})$ is to estimate two unknown variables $\boldsymbol{A}$ *and* $\boldsymbol{t}(\boldsymbol{z})$. The author proposed a simple but effective solution in the previous paper [8].

Since the *skylight* $\boldsymbol{A}$ equals the *airlight* coming from infinite $d = \infty$ with highest scattering, it's extracted from the luminance image $Y(\boldsymbol{z})$ of $\boldsymbol{I}(\boldsymbol{z})$. Applying a local minimum filter to $Y(\boldsymbol{z})$, we get

$$Y^{\text{dark}}(\boldsymbol{z}) = \left\{ \min_{\boldsymbol{w} \in \boldsymbol{\Omega}(\boldsymbol{z})} (Y(\boldsymbol{w})) \right\}. \tag{2}$$

The local ***min*** block filter substitutes the darkest value for pixel $\boldsymbol{w}$ inside each sub-divided block area Ω. As a result, the blocks for the scattered *airlight* hard to reach are omitted from the candidates.

Thus the *skylight* $\boldsymbol{A}$ is estimated by extracting the brighter area Ω_{Sky} and taking the average as

$$\tilde{\boldsymbol{A}} = \text{mean}_{\boldsymbol{w} \in \Omega_{\text{Sky}}(\boldsymbol{z})} \{\boldsymbol{I}(\boldsymbol{w})\} \quad \text{for } \Omega_{\text{Sky}}(\boldsymbol{z}) = \text{area} \left\{ Y^{\text{dark}}(\boldsymbol{z}) \geq Y_H \right\}. \tag{3}$$

Normalizing Eq. (1) by the estimated *skylight* $\tilde{\boldsymbol{A}}$, it's eliminated from the 2nd term as

$$I^C_{\text{Norm}}(\boldsymbol{z}) = \frac{I^C(\boldsymbol{z})}{\tilde{A}^C} = \frac{J^C(\boldsymbol{z})}{\tilde{A}^C} t(\boldsymbol{z}) + (1 - t(\boldsymbol{z})) \quad \text{for } C{=}R, G, B. \tag{4}$$

Operating DCP (Dark Channel Prior) [14] process on Eq. (4) and introducing a *veiling factor* α $(0 < \alpha < 1)$, the scene transmittance $\boldsymbol{t}(\boldsymbol{z})$ is roughly estimated from the 2nd term in Eq. (4) as

$$\tilde{t}(\boldsymbol{z})^{\text{rough}} \cong 1 - \alpha \left\{ \min_{C \in \{R,G,B\}} \frac{I^C(\boldsymbol{z})}{A^C} \right\}. \tag{5}$$

Because the scene transmittance should be spatially continuous and smooth, it's refined by Bilateral Filter as

$$\tilde{\boldsymbol{t}}(\boldsymbol{z})^{\text{smooth}} = \text{Bilateral Filter}[\tilde{\boldsymbol{t}}(\boldsymbol{z})^{\text{rough}}]. \tag{6}$$

Once the *skylight* $\boldsymbol{A}$ and *scene transmittance* $\boldsymbol{t}(\boldsymbol{z})$ are estimated, the scene *albedo* is recovered from Eq. (1) as

$$\tilde{\boldsymbol{\rho}}(\boldsymbol{z}) \cong \tilde{\boldsymbol{J}}(\boldsymbol{z})/\tilde{\boldsymbol{A}} = (\boldsymbol{I}(\boldsymbol{z})/\tilde{\boldsymbol{A}} - 1 + \tilde{\boldsymbol{t}}(\boldsymbol{z}))/\text{Max}[\tilde{\boldsymbol{t}}(\boldsymbol{z}), t_0], \tag{7}$$

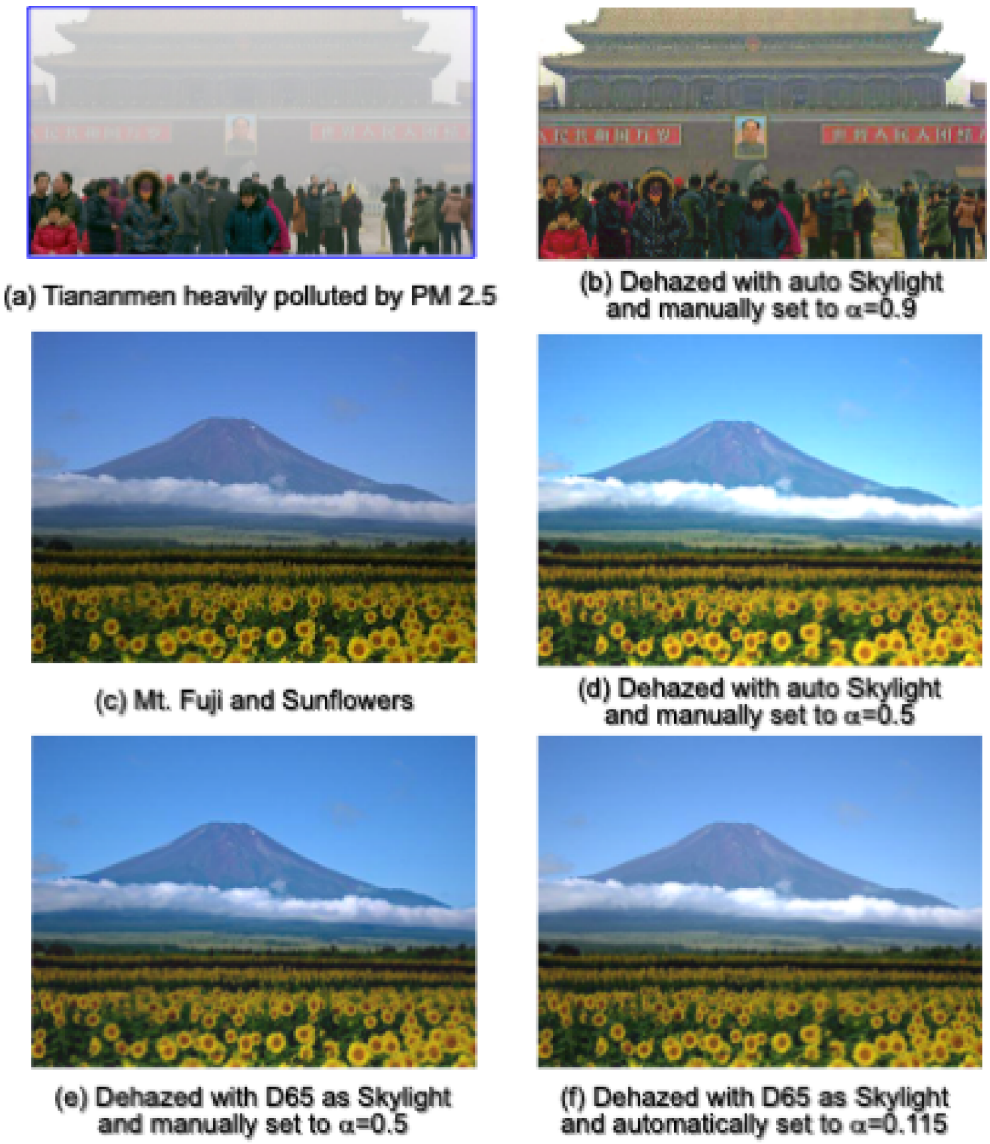

Figure 2. Dehazed samples by selecting skylight $\boldsymbol{A}$ and tuning veiling factor α.

where, Max [,] is a limiter to take $\tilde{t}(\boldsymbol{z}) \geq t_0$ in case of the very low transmittance pixel point for the *albedo* $\tilde{\boldsymbol{\rho}}(\boldsymbol{z})$ not to diverge.

Usually, the veiling factor is set around $\alpha = 0.9$ or higher to perfectly unveil the scattered *airlight*. While, the *α-based Dehazing* works to regulate the scene transmittance $\tilde{t}(\boldsymbol{z})$ to at least 1-α. By adjusting the veiling factor α to the lower value, it'll be used for thin-hazed daily scenes. The *veiling factor* α is unresolved, but is roughly estimated by subtracting the spatial average of the scene transmittance of Eq. (6) from 1.0 (transparency 100%) and used as a guide for α like as,

$$\begin{aligned} \alpha &\cong 1 - \text{mean}[\tilde{\boldsymbol{t}}(\boldsymbol{z})^{\text{smooth}}] \\ &= 1 - \left(\frac{1}{WH}\right) \sum_{x=1,y=1}^{x=W,y=H} \tilde{\boldsymbol{t}}(x,y)^{\text{smooth}} \end{aligned} \tag{8}$$

for the image size of width W and height H.

Another important factor with *veiling factor* α is the *skylight* $\boldsymbol{A}$, which illuminates the scene.

Figure 2 shows a *dehazed* example applied to two typical scenes by tuning α and setting the *skylight* $\boldsymbol{A}$. One is Tiananmen Square heavily degraded by PM 2.5 air-pollution, the other is a little hazy Mt. Fuji. The *dehazing* for the daily scenery Mt. Fuji may not be necessary, but we tested it to verify the proposed model.

In the *dehazing* result (b) for (a), the *skylight* $\boldsymbol{A}$ is automatically detected by Eq. (3), and α is manually set to 0.9 from the empirical value. The heavy PM 2.5 air-pollution has been dramatically removed and the Tiananmen Building with Mao Zedong panel is clearly visible.

On the other hand, in the dehazing result (d) for Mt. Fuji (c), the *skylight* $\boldsymbol{A}$ is automatically detected, but α is manually set to 0.5 as an appropriate guideline. The clear blue sky and the view of sunflower field seem to have improved. However,

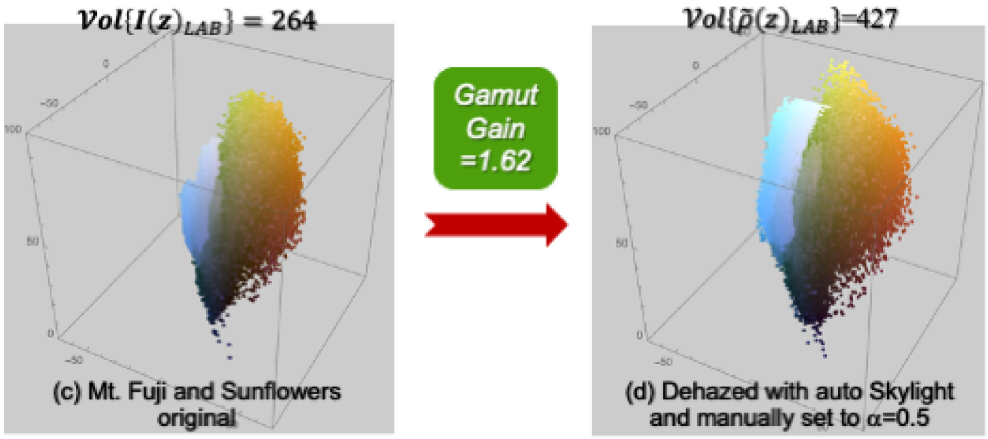

Figure 3. Gamut expansion effect by Dehazing for the case of Fig. 2(d).

the cyanish sky blue is a little unnatural and the shadows of the white clouds may be a bit lost. Therefore, in (e), the *skylight* $\boldsymbol{A}$ is set as the standard D65 light source, and in (f), α is automatically set by Eq. (8). Which of (d), (e), and (f) is preferable is controversial, and we have no grand truth. Development of evaluation method is a future task.

4. DEHAZING EFFECTS

4.1 *Color Gamut Expansion*

Since the haze-free true scene is unknown, it has been difficult to measure the *Dehazing* effects in material appearance.

Though, by unveiling the scattered light through haze mist, or pollution, the effect is reflected to recover the clear scene color reproduction. As a result, the scene color gamut is expanded. Hence the effect can be measured by how the color gamut volume is expanded before and after *Dehazing*. Here, the volume of solid color is numerically estimated by ellipsoidal approximation using PCA (Principal Component Analysis).

The volume of the CIELAB color distribution $\boldsymbol{I}(\boldsymbol{z})_{\mathrm{LAB}}$ of the original image $\boldsymbol{I}$ $(\boldsymbol{z})$ is calculated by the following equation.

$$\boldsymbol{Vol}\{\boldsymbol{I}(\boldsymbol{z})_{\mathrm{LAB}}\} = (4\pi/3)\sqrt{\lambda_1}\sqrt{\lambda_2}\sqrt{\lambda_3} \tag{9}$$

$$\boldsymbol{\lambda} = \{\lambda_1, \lambda_2, \lambda_3\} = \boldsymbol{Eigenvalue}\{\boldsymbol{I}(\boldsymbol{z})_{\mathrm{LAB}}\} \tag{10}$$

where, $\{\lambda_1, \lambda_2, \lambda_3\}$ represent the eigenvalues of the first, second and third principal components.

The volume $\boldsymbol{Vol}\{\tilde{\boldsymbol{\rho}}(\boldsymbol{z})_{\mathrm{LAB}}\}$ of CIELAB color solid for restored albedo is also calculated in the same manner. Hence, the volume ratio of the color solids for the images before and after Dehazing is changed to the *Gamut Gain* can be used as a measure of the effect of Dehazing as

$$\boldsymbol{Gamut\,Gain} = \boldsymbol{Vol}\{\tilde{\boldsymbol{\rho}}(\boldsymbol{z})_{\mathrm{LAB}}\}/\boldsymbol{Vol}\{\boldsymbol{I}(\boldsymbol{z})_{\mathrm{LAB}}\}, \tag{11}$$

Figure 3 demonstrates an example in which the dehazing effect of Mt. Fuji in Fig. 2 above was evaluated by Gamut Gain. In this sample, the volume of color solid has been stretched about 1.6 times by Dehazing.

4.2 *Air Clarity Enhancement*

The α-based Dehazing can be applied to daily scenes with almost no haze, and can be used to emphasize a sense of clarity. Now a question may arise if the *skylight* $\boldsymbol{A}$ is safely detected or not for a scene without sky. When the scene is taken by sRGB camera, the *skylight* $\boldsymbol{A}$ may be preset to D65. Even in a scene without sky, if the sunlight is detected through the trees, *Dehazing* is possible. Figure 4 is a common scene without sky. The detected *skylight* area is marked in red circled. The *veiling factor* is estimated as $\alpha \cong 0.09$, which indicates about 9% should be dehazed. In this sample, fortunately, the *skylight* $\boldsymbol{A}$ was successfully detected, so the effect of removing $\boldsymbol{A}$ by Eq. (4) is valuable, and the actual *Dehazing* effect may be rather small, since the amount of haze was estimated as 9%. Though, the scene visibility of estimated albedo $\tilde{\boldsymbol{\rho}}(\boldsymbol{z})$ is obviously much improved better than the original. At the same time, in this sample, the volume of color gamut has been stretched about 2.5 times by Dehazing.

4.3 *Wetness Enhancement*

Sawayama and Nishida developed a ***Wet filter*** which creates a ***wet*** feeling by making the original image highly saturated and adding distortion (*skew*) to the luminance histogram. It succeeded in giving a wet feeling to the dry stones of a riverbank. The idea of *skew* may seem "*heuristic*" and little bit *illogical*, but it would be a gift of great imagination. The effect of ***Wet filter*** is statistically verified by evaluation experiments [15].

Our α*-based Dehazing* has both functions of air clarity enhancement and a color correction at the same time. We also noticed that adjusting the veil coefficient α creates a wet feeling by a kind of *Skew* effect and found that the wet feeling can be further amplified by adjusting the *gamma coefficient* γ of sRGB display.

Figure 5 shows an example of α*-based Dehazing* with *modified* display *gamma* in comparison with ***Wet filter***. As an intuitive trial, a Dehazed image is displayed by just changing the sRGB *gamma* to $\gamma = 0.7$ from $\gamma = 1/2.2$ (standard). This trial also seems "*tricky*" but resulted in a similar feeling to that by ***Wet filter***.

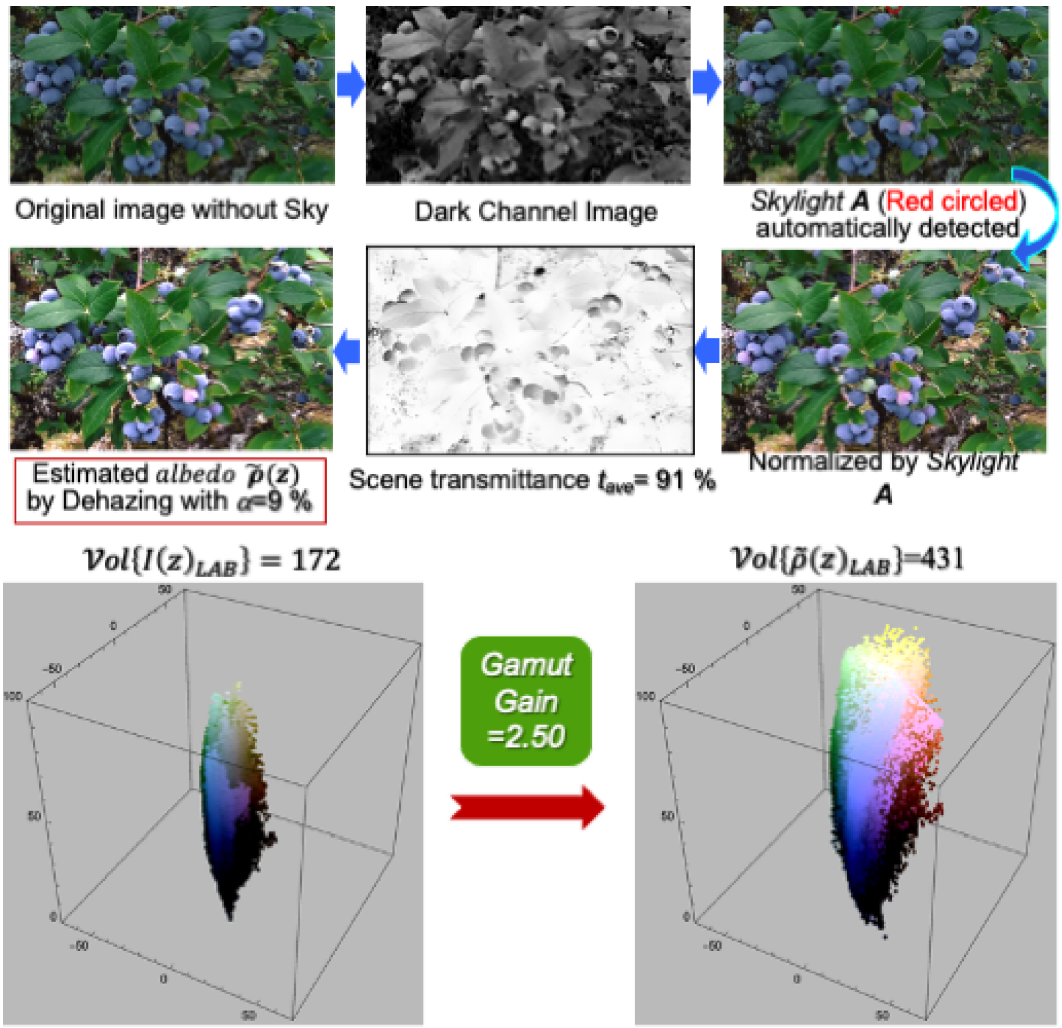

Figure 4. Dehazing effects in clarity enhancement and gamut expansion for a scene without sky.

4.4 *Gloss Enhancement*

The α-*based Dehazing* resulted in unexpected effect in ***gloss*** enhancement. Figure 6 is a comparison with the "***gloss***" control method developed by Kobiki et al. [6] based on the concept of BRDF. The original "Tomato" image is a special example of hue-biased to "*Red*" and the luminance concentrated to lower level as shown in the luminance Y histogram. They succeeded in the separation of "*specular*" component $\boldsymbol{S}$ using this biased hue distribution and controlled "***gloss***" without measuring BRDF. The proposed model is clearly superior to BRDF in that it reproduces the "*Green*" in dark calyx, which is basically a unique function of *Dehazing* that one can never achieve with BRDF. Our automatic estimation algorithm for *skylight* and scene *transmittance* leads to the reproduction of ***color*** and ***gloss*** at the same time.

4.5 β-*based Contrast Model: LCGT*

Tone Mapping Operator (TMO) plays an important role in reproducing ***texture*** and/or ***roughness*** on the surface of objects. TMO is classified to the following two types [16].

type-1 Spatially-invariant Global TMO

type-2 Spatially-variant Local TMO

Spatially-invariant TMO operates point-wise tone mapping on all of the pixels independent of spatial coordinates based on the global adaptation of vision. On the other hand, Spatially-variant TMO applies an image-dependent spatial tone mapping to improve the local visual contrast. Since the ***type-2*** operators realize flexible mappings, they are becoming mainstream in recent years.

In this article, a vision-based ***type-2*** TMO, *LCGT* operator [10] is adopted to enhance the appearance for ***texture*** and ***roughness*** of the surface of object.

The conceptual model of *LCGT* is illustrated in Figure 7.

Weber fraction is a well-known contrast measure for the change of intensity in the center vs. surround $\Delta I/I$. Based on the nonlinear response of human vision system, the *Weber fraction* is defined by the differential of the logarithm of intensity as [17]

$$C_W \cong \Delta I/I = d\{\log(I)\} = dI/I. \tag{12}$$

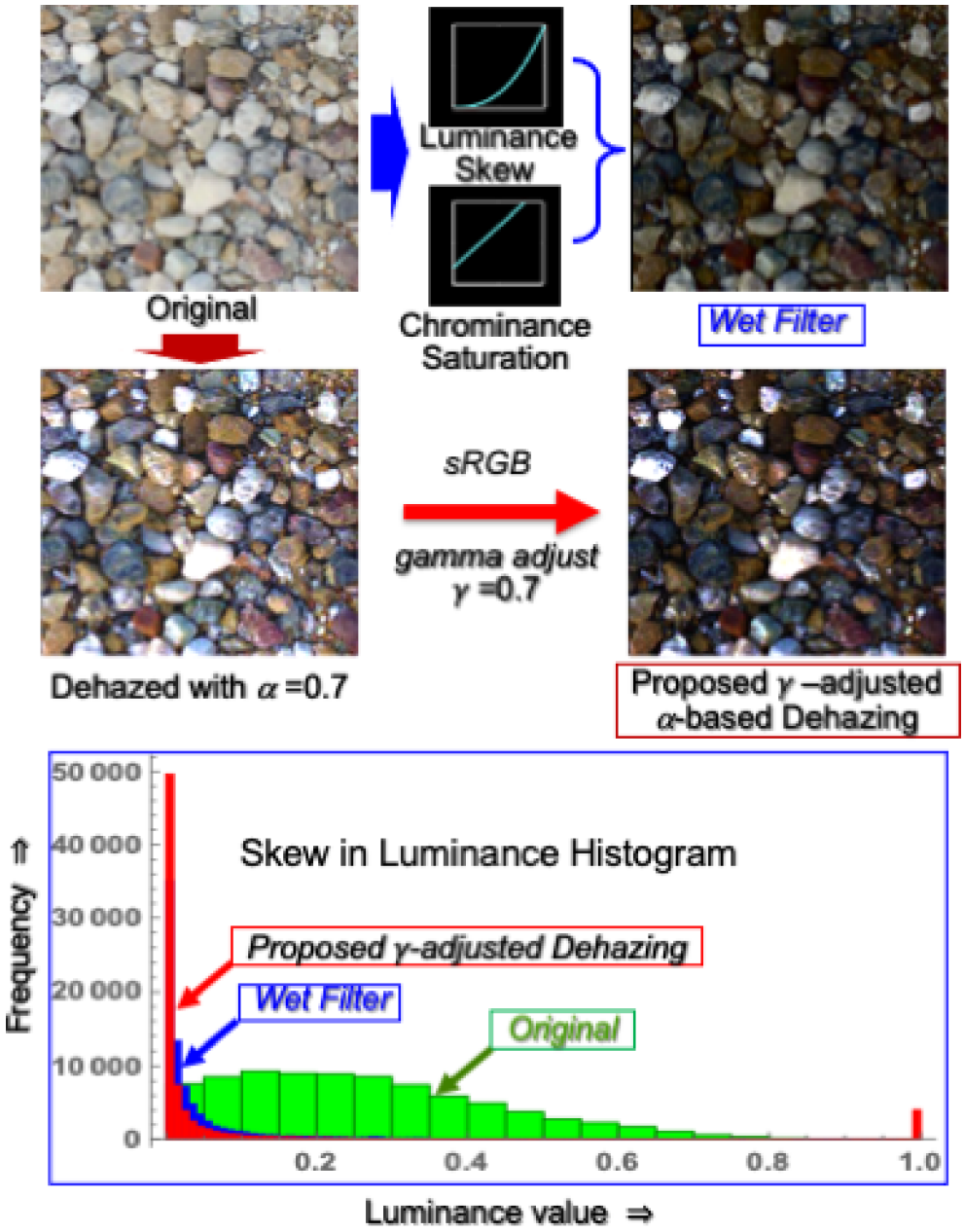

Figure 5. Wetness enhancement and Skew effect in luminance histogram by modified α-based Dehazing model in comparison with Wet filter.

Here, the Weber Contrast gain WC_{gain} is defined by the ratio of Weber fraction C_{Wg} of output $g(x,y)$ vs. C_{Wf} of input $f(x,y)$ as

$$WC_{\text{gain}}(x,y) = \frac{C_{Wg}}{C_{Wf}} = \frac{dg(x,y)/g(x,y)}{df(x,y)/f(x,y)} = \frac{dG(x,y)}{dF(x,y)} \tag{13}$$

$F(x,y)$ and $G(x,y)$ mean the logarithm of input image $f(x,y)$ and output image $g(x,y)$. Hence WC_{gain} equals dG/dF that signifies the slope of input vs. output in logarithmic space.

Considering the system TRC (Tone Reproduction Curve)

$$g(x,y) = \text{TRC}\{f(x,y)\}. \tag{14}$$

Eq. (10) is rewritten by the following formula

$$WC_{\text{gain}}(x,y) = \frac{f(x,y)}{\text{TRC}(f(x,y))} \cdot \frac{d\text{TRC}(f(x,y))}{df(x,y)}. \tag{15}$$

The condition that the average output traces just on the given TRC to maintain the smoothed tonal mapping is given by

$$g_{\text{ave}}(x,y) = \text{TRC}(f_{\text{ave}}(x,y)). \tag{16}$$

Solving Eq. (13) in case of the ideal linear TRC, we get

$$g(x,y) = \text{TRC}(f_{\text{ave}}(x,y)) \cdot \left(\frac{f(x,y)}{f_{\text{ave}}(x,y)}\right)^{WC_{\text{gain}}}, \tag{17}$$

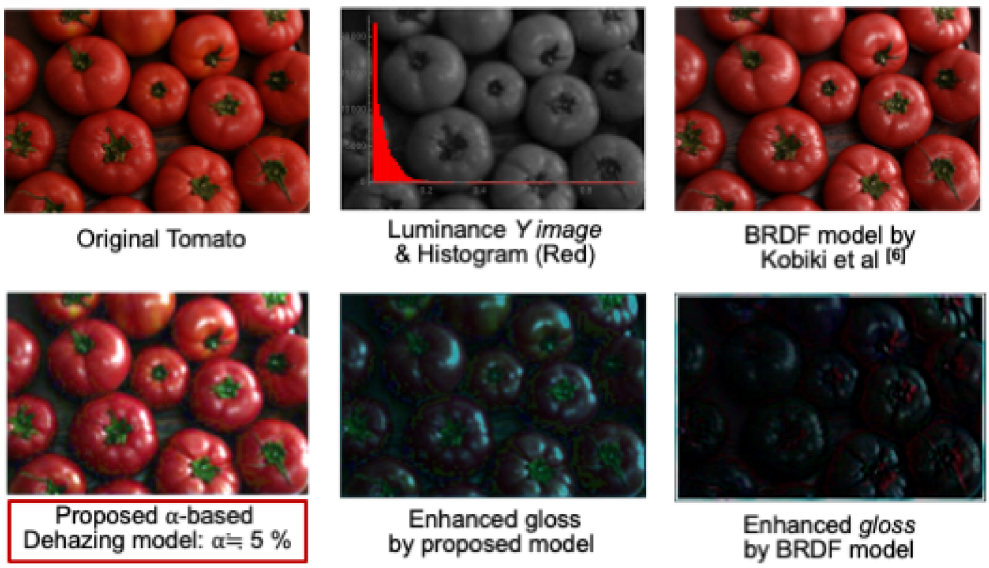

Figure 6. Gloss enhancement by α-based Dehazing model in comparison with conventional BRDF model.

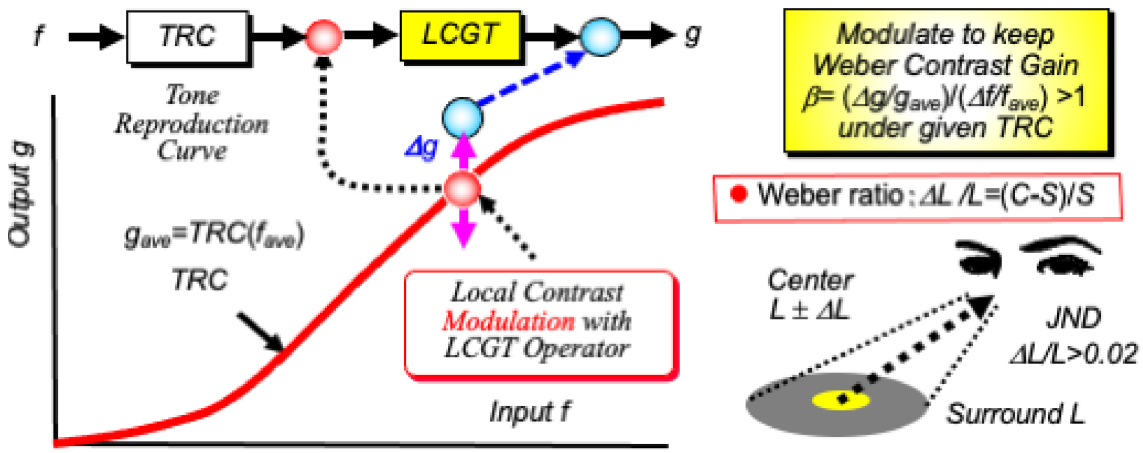

Figure 7. Local Contrast Enhancement System based on Weber's law.

where, (f/f_{ave}) means C/S (Center/Surround) ratio of the input image and the surround $f_{\text{ave}}(x,y)$ is given by a Gaussian average.

Now, setting the Weber Contrast gain to be a constant value of $WC_{\text{gain}}(x,y) = \beta > 1$, we get a simple solution as

$$g(x,y) = \text{TRC}\{f_{\text{ave}}(x,y)\} \cdot \left(\frac{f(x,y)}{f_{\text{ave}}(x,y)}\right)^{\beta}. \qquad (18)$$

This denotes a power function of β and works to enhance the local contrast keeping $\beta > 1$ everywhere and tracing on the given TRC of system not to deviate from it.

4.6 *Texture and Roughness Enhancement*

Figure 8 shows typical examples of appearance enhancement for ***texture*** and ***roughness*** on the surface of objects by *LCGT* in comparison with *Band Shift* model [18].

The *Band Shift* model decomposes the spatial frequency component of an image into multiple sub-bands according to the high and low frequencies and the strength of the component. Then the appearance of ***texture*** and ***roughness*** are controlled by emphasizing or reducing each of them and synthesizing them. There are many combinations of sub-band selection, emphasis or mitigation, and the results are intuitively adopted, so it depends on the user's preference. On the other hand, the proposed model is simple and rational because it is controlled only by the gain parameter β based on the visual model.

Figure 9 shows the distribution of the *DCT* Fourier amplitude spectrum of the increased ΔL of luminance component after contrast enhancement when $\beta = 3$. It shows that the spectra around **3 to 12 *cpd***, sensitive to human vision, are effectively emphasized.

4.7 *Cooperative Effect of α-based Dehazing and β-based Contrast Models*

Finally, the cooperative effect of the above two models of *α-based Dehazing and β-based Contrast are examined.*

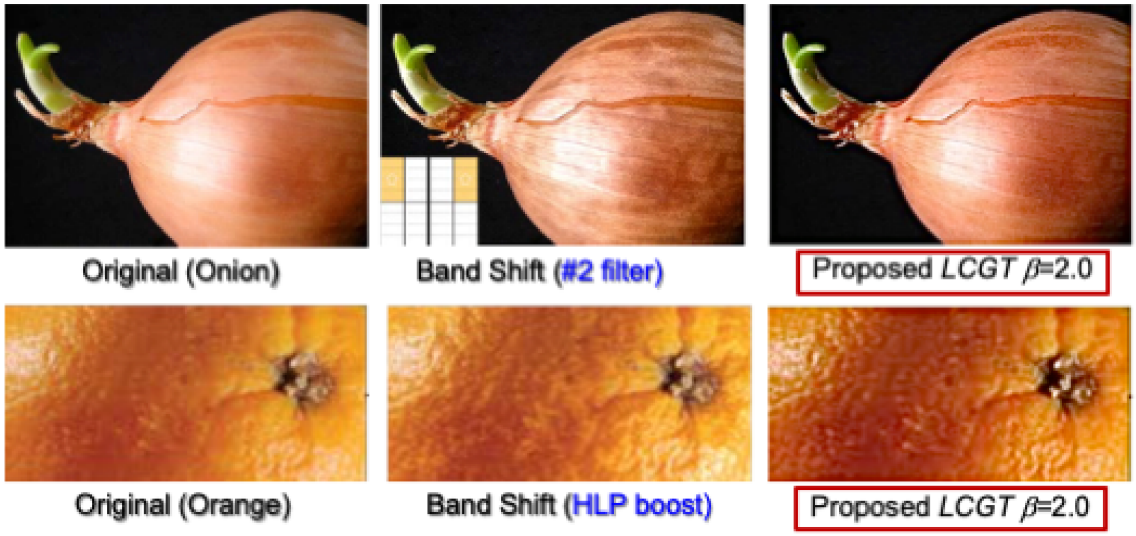

Figure 8. Texture and roughness enhancement by gain β with LCGT.

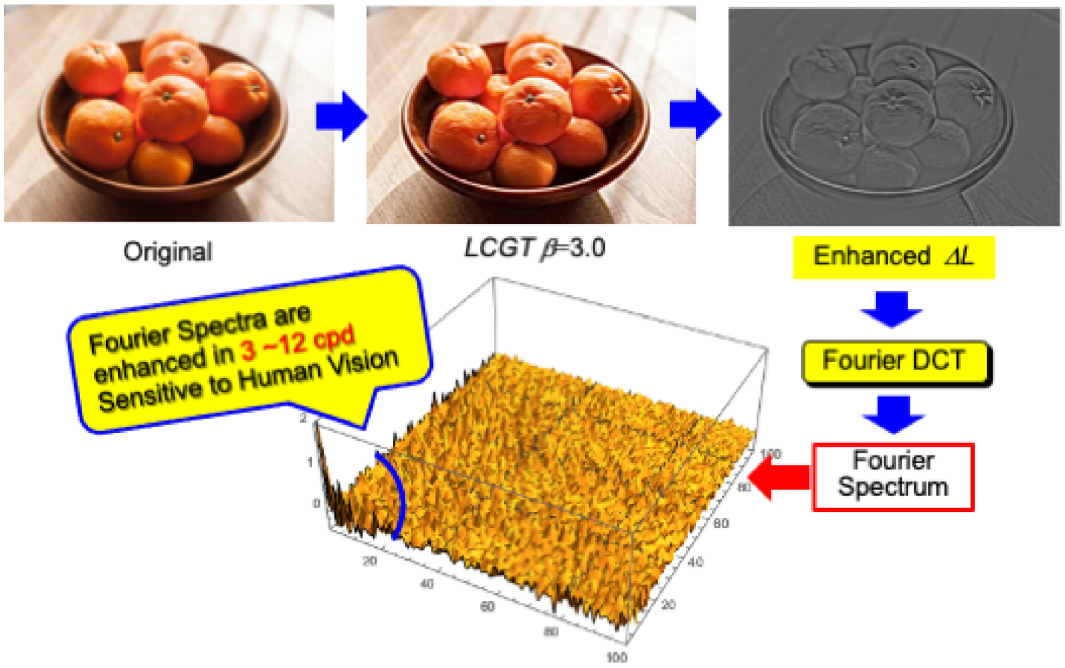

Figure 9. Fourier Spectra distribution of increased luminance by LCGT.

Figure 10 is a sample that LCGT plays a leading role in enhancing the meshes of "Melon", while Dehazing plays a supporting role. It contributes to reproduce slightly clear colors.

On the contrary, in Figure 11, the Dehazing works effectively to recover the clear colors of "Pebble on beach" with the air clarity. By the cooperation with LCGT, the pebble's texture and colors appear to be revived along with a feeling of scene transparency.

However, in this example, the highlight part of the original image is slightly overexposed, so the detection of skylight was ambiguous and the veiling factor α might be underestimated. Here, α is manually preset to 0.7 based on experience points.

We have verified that *a-based Dehazing* works well in many cases, but it depends on the imaging conditions and the scene, and further improvement is necessary for stabilization.

5. CONCLUSIONS

SHITSUKAN (material perception/appearance) research is a profound science. Since the perceptual phenomena involve many complicated factors related to optics, vision, neuroscience, psychology, and brain science, it's difficult to unravel what and how our brain feels from the retinal images.

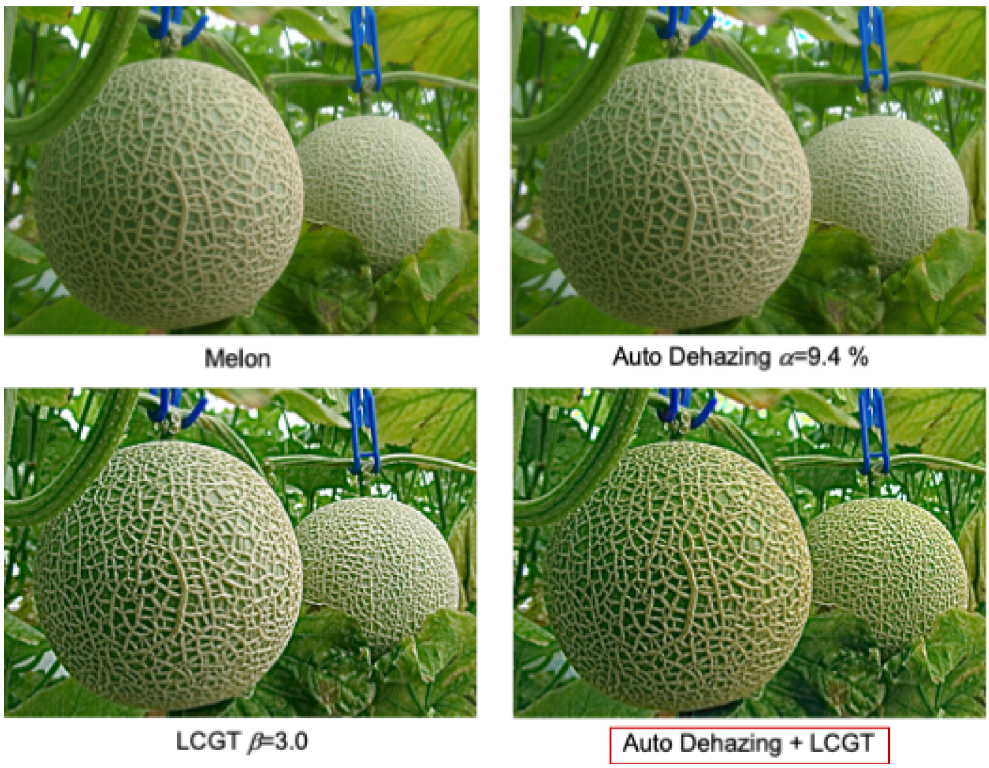

Figure 10. Sample: LCGT leading and Dehazing supporting.

Hence, the heuristic or intuitive approaches have been attempted. The proposed *α-based Dehazing* may be one of these heuristic approaches. Though *Dehazing* has been mostly applied to heavy air polluted scenes, it proved useful for daily natural scenes by adjusting the *veiling factor* α, even if the objects placed at a short distance.

This study also introduced a vision-based local contrast enhancement operator *β-based LCGT* based on Weber fraction theory. It has worked well for enhancing the surface textural appearances.

In practice, both *α-based Dehazing* and *β-based LCGT* showed individual advantages for enhancing the material appearances such as {"***air clarity***", "***wetness***", "***gloss***"} and {"***texture***", "***roughness***"} together with mutual cooperation effects. Particularly, *α-based Dehazing* recovers the vivid object colors and the traces of "***gloss***" information are reflected to its scene transmission map. Towards future *SHITUKAN* research, it'll be the ultimate goal to answer the question "***how the brain feels beauty***?" asked repeatedly by Semir Zeki in his book, INNER VISION [19].

6. DISCUSSION AND FUTURE WORK

Human vision can recognize material property at a glance. Without touching the objects, we can tell whether the materials would be hard or soft, cool or warm, rough or smooth, wet or dry. Furthermore, it is possible to determine whether the material is metal or wood, synthetic leather or real leather. The material appearance is interpreted as a perceptual phenomenon of feeling or sensation that our brain perceives from optical image in retina. Though, it's hard to untangle what information of the retinal image stimulates the visual cortex and how it induces the material perception in our brain. The mechanism of INNER VISION is still a black box at present.

Despite the difficulties, material appearance researches have greatly progressed over the last few years. These are the following development examples.

- Perceptual quality evaluation and material classification using photographs of various materials [20].
- Systematic prediction model of material perception based on interaction between lighting and materials [21].
- Perceptual roughness analysis of glossy objects considering Fresnel effect and Fresnel-BRDF correction model [22].
- Optical mixing method to probe visual material perception [23].
- The effect of shape and illumination on material perception: model and applications [24].

The proposed study remains at the stage of simulation based on a mathematical model, and psychophysical evaluation experiments by human subjects have not been conducted yet and are planned for future work. With reference to the above studies, we want to continue further research and tackle the quantitative evaluation method of texture and the improvement in visual appearance by emphasis.

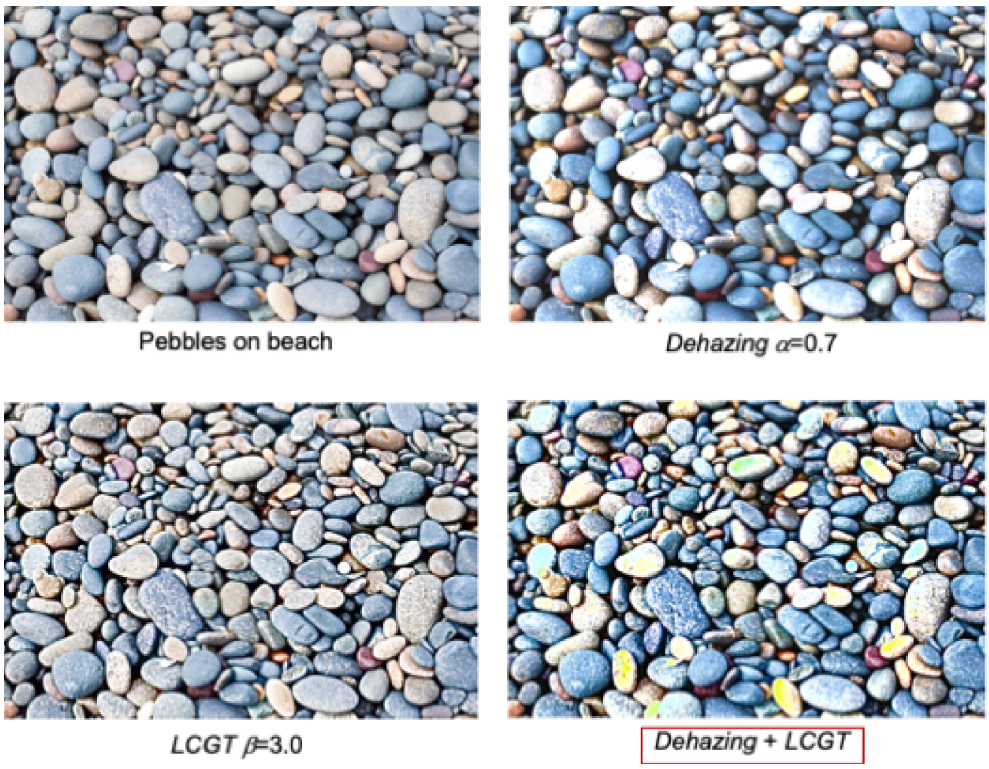

Figure 11. Sample: Dehazing leading and LCGT supporting.

REFERENCES

[1] R. W. Fleming, "Visual perception of materials and their properties," Vis. Res. **94**, 62–75 (2014).

[2] N. Tsumura, K. Baba, S. Yamamoto, and M. Sambongi, "Estimating reflectance property from refocused images and its application to auto material appearance balancing," J. Imaging Sci. Technol. **59**, 030501-1–030501-6 (2015).

[3] http://shitsukan.jp.

[4] I. Motoyoshi, S. Nishida, L. Sharan, and E. H. Adelson, "Image statistics and the perception of surface qualities," Nature **447**, 206–209 (2007).

[5] M. Sawayama and S. Nishida, "Visual perception of surface wetness," J. Vis. **15**, 937–937 (2015).

[6] H. Kobiki, R. Nonaka, and M. Baba, "Specular reflection control technology to increase glossiness of images," Toshiba Rev. **68**, 38–41 (2013).

[7] H. Kotera, "Material appearance transfer with visual cortex image," *Proc. CCIW 2019* (Springer, Berlin, 2019), pp. 334–348.

[8] H. Kotera, "Unveiling PM 2.5 pollution layer for viewing clear scenes," *Proc. IS&T CIC22: Twenty-second Color and Imaging Conf.* (IS&T, Springfield, VA, 2014), pp. 59–64.

[9] H. Kotera, "Scene color correction under non-uniform spatial illumination and atmospheric transmittance," *Proc. IS&T CIC24: Twenty-fourth Color and Imaging Conf.* (IS&T, Springfield, VA, 2016), pp. 300–305.

[10] H. Kotera, T. Horiuchi, R. Saito, H. Yamashita, and Y. Monobe, "Visual contrast mapping based on Weber's fraction," *Proc. IS&T/SID CIC14: Fourteenth Color Imaging Conf.* (IS&T, Springfield, VA, 2006), pp. 257–262.

[11] Y. Monobe, H. Yamashita, T. Kurosawa, and H. Kotera, "Dynamic range compression preserving local image contrast for digital video camera," IEEE Trans. Consum. Electron. **51**, 1–11 (2005).

[12] H. Yamashita, Y. Monobe, T. Kurosawa, and H. Kotera, "Contrast-gain-based visual tone mapping for digital photo prints," J. Imaging Sci. Technol. **50**, 458–468 (2006).

[13] S. Narasimhan and S. Nayar, "Vision and atmosphere," J. Comput. Vis. **48**, 233–254 (2002).

[14] K. He, J. Sun, and X. Tang, "Single image haze removal using dark channel prior," *Proc. IEEE Computer Vision Pattern Recognition* (IEEE, Piscataway, NJ, 2009), pp. 1956–1963.

[15] M. Sawayama, E. H. Adelson, and S. Nishida, "Visual wetness perception based on image color statistics," J. Vis. **17(5)**, 1–24 (2017).

[16] E. Reinhard, W. Heidrich, P. Debevec, S. Pattanaik, G. Ward, and K. Myszkowski, *High Dynamic Range Imaging* (Morgan Kaufmann Publisher, Burlington, Massachusetts, 2006).

[17] W. K. Pratt, *Digital Image Processing* (John Wiley & Sons, Inc., Hoboken, New Jersey, 1978).

[18] I. Boyadzhiev, K. Bala, S. Paris, and E. H. Adelson, "Band-shifting decomposition for image-based material editing," ACM Trans. Graph. **34**, 1–16 (2015).

[19] S. Zeki, *INNER VISION: An Exploration of Art and the Brain* (Oxford University Press, Oxford, England, 1999).

[20] R. W. Fleming, C. Wiebel, and K. Gegenfurtner, "Perceptual qualities and material classes," J. Vis. **13**, 9 (2013).

[21] F. Zhang, H. de Ridder, P. Barla, and S. Pont, "A systematic approach to testing and predicting light-material interactions," J. Vis. **19**, 11 (2019).

[22] F. Faul, "Perceived roughness of glossy objects, "The influence of Fresnel effects and correlated image statistics"," J. Vis. **21**, 1 (2021).

[23] F. Zhang, H. de Ridder, R. W. Fleming, and S. Pont, "MatMix 1.0: using optical mixing to probe visual material perception," J. Vis. **16**, 11 (2016).

[24] A. Serrano, B. Chen, C. Wang, M. Piovarči, H. P. Seidel, P. Didyk, and K. Myszkowski, "The effect of shape and illumination on material perception: model and applications," ACM Trans. Graph. **40**, 4 (2021).